

Chlorine atom formation dynamics in the dissociation of $\text{CH}_3\text{CF}_2\text{Cl}$ (HCFC-142b) after UV laser photoexcitation

Richard A. Brownsword, Patricia Schmiechen, and Hans-Robert Volpp^{a)}
*Physikalisch-Chemisches Institut der Universität Heidelberg, Im Neuenheimer Feld 253,
D-69120 Heidelberg, Germany*

Hari P. Upadhyaya
Chemistry Division, Bhabha Atomic Research Centre, Bombay 400-085, India

Young Jae Jung^{a)} and Kyung-Hoon Jung
*Center for Molecular Science and Department of Chemistry, Korea Advanced Institute of Science
and Technology, Taeduck Science Town, Taejon 305-701, Korea*

(Received 8 December 1998; accepted 30 March 1999)

The dynamics of chlorine atom formation after UV photoexcitation of $\text{CH}_3\text{CF}_2\text{Cl}$ (HCFC-142b) in the gas phase was studied by a pulsed laser photolysis/laser-induced fluorescence (LIF) “pump-and-probe” technique at room temperature. The parent molecule was excited at the ArF excimer laser wavelength (193.3 nm) and nascent ground state $\text{Cl}(^2P_{3/2})$ and spin-orbit excited $\text{Cl}^*(^2P_{1/2})$ photofragments were detected under collision-free conditions via laser induced fluorescence in the vacuum ultraviolet spectral region. Narrow-band probe laser radiation, tunable over the wavelength range 133.5–136.4 nm, was generated via resonant third-order sum-difference frequency conversion of dye laser radiation in Krypton. Using HCl photolysis at 193.3 nm as a source of well-defined $\text{Cl}(^2P_{3/2})$ and $\text{Cl}^*(^2P_{1/2})$ concentrations, values for the total Cl atom quantum yield ($\Phi_{\text{Cl}+\text{Cl}^*}=0.90\pm 0.17$) and the $[\text{Cl}^*]/[\text{Cl}]$ branching ratio 0.39 ± 0.11 were determined by means of a photolytic calibration method. From the measured Cl and Cl^* atom Doppler profiles the average relative translational energy of the fragments could be determined to be 125 ± 25 kJ/mol. The corresponding value $f_T=0.48\pm 0.10$ of the fraction of total available energy channeled into product translational energy was found to be (within experimental uncertainty) in agreement with the result $f_T=0.39$ of a dynamical simulation assuming a repulsive model for single C–Cl bond cleavage. Both the measured total Cl atom quantum yield and the energy disposal indicates that direct C–Cl bond cleavage is a primary fragmentation mechanism for $\text{CH}_3\text{CF}_2\text{Cl}$ after photoexcitation at 193.3 nm. © 1999 American Institute of Physics. [S0021-9606(99)00624-8]

I. INTRODUCTION

As a consequence of the Copenhagen Amendment of the Montreal Protocol, which allows the use of hydrochlorofluorocarbons (HCFCs), on a transitional basis, as replacements of the ozone-destroying chlorofluorocarbons (CFCs),¹ it can be expected that the atmospheric HCFC concentrations will continue to increase rapidly over the next years. Although HCFC compounds, which have at least one C–H bond, can be oxidized by OH free radicals and $\text{O}(^1D)$ atoms in the troposphere,² they still have the potential to lead to significant chlorine transportation to the stratosphere³ where they are destroyed by photochemical processes initiated by light absorption in the 190–230 nm wavelength region.⁴ In addition, HCFCs, like CFCs, absorb long-wavelength radiation and should therefore also be considered as potential greenhouse gases.⁵ In recent measurements of stratospheric profiles of $\text{CH}_3\text{CF}_2\text{Cl}$ (HCFC-142b), which has been used since the late 1980s to replace CF_2Cl_2 (CFC-12) as a foam blowing agent in industry,⁶ it was found that $\text{CH}_3\text{CF}_2\text{Cl}$ is not yet in equilibrium, due to its rapidly increasing emissions.^{7,8} There-

fore besides atmospheric concentration measurements and advanced 3D modeling calculations,⁹ laboratory photodissociation dynamics studies of HCFCs and in particular quantitative measurements of primary photochemical product yields are needed to assess their environmental impact.¹⁰

For a number of HCFCs, optical absorption spectra in the infrared (IR), ultraviolet (UV), and vacuum-ultraviolet (VUV) spectral region were measured.^{5,11} Pyrolysis¹² and decomposition of chemically activated¹³ $\text{CH}_3\text{CF}_2\text{Cl}$ as well as the infrared multiple photon decomposition (IRMPD)^{14,15} of $\text{CH}_3\text{CF}_2\text{Cl}$ was studied in detail. The results of these studies indicate that decomposition on the ground state electronic potential energy surface (PES) can be characterized by a four-center unimolecular elimination pathway leading to $\text{CH}_2=\text{CF}_2+\text{HCl}$ as major products and to a minor extent to $\text{CH}_2=\text{CFCl}+\text{HF}$ products.

Early gas-phase photodecomposition studies of $\text{CH}_3\text{CF}_2\text{Cl}$ after irradiation with VUV light (147 nm;¹⁶ 123.6 nm¹⁷) were carried out under static conditions as a function of irradiation time (30–180 min), $\text{CH}_3\text{CF}_2\text{Cl}$ pressure (3.6–20.6 Torr) and/or in the absence and presence of radical scavenging agents (NO , H_2S , HI) with stable end-product analysis (CH_2CF_2 , CH_2CHF , C_2H_2 , CH_4 , and CH_3Cl) being

^{a)} Authors to whom correspondence should be addressed.

performed by flame ionization gas chromatography. Only recently laser-based $\text{CH}_3\text{CF}_2\text{Cl}$ low-pressure gas-phase photolysis experiments have been carried out in which primary photochemical product yields could be determined under collision-free conditions.^{18,19} In Ref. 18, the H atom formation dynamics after UV (193.3 nm) and VUV (121.6 nm) laser excitation was investigated and absolute quantum yields Φ_{H} for H atom formation were reported. The measured values of $\Phi_{\text{H}}(193.3 \text{ nm})=0.06\pm 0.02$ and $\Phi_{\text{H}}(121.6 \text{ nm})=0.53\pm 0.12$ indicate the increasing importance of the H atom formation pathway in the $\text{CH}_3\text{CF}_2\text{Cl}$ fragmentation in going from UV to VUV excitation wavelengths. In Ref. 19, H atom, ground state $\text{Cl}(^2P_{3/2})$ and spin-orbit excited $\text{Cl}^*(^2P_{1/2})$ atoms, and HCl product formation were investigated after laser excitation at 193.3 nm. Using time-of-flight mass spectrometry (TOF-MS) in combination with (2+1) resonance-enhanced multiphoton ionization (REMPI) for product detection H, Cl, and Cl^* atom formation was observed. In these experiments, no $\text{HCl}(v''=0,1)$ product molecules could be detected and an upper limit of 1% ($\Phi_{\text{HCl}(v''=0,1)}(193.3 \text{ nm})<0.01$) was estimated for the HCl elimination channel. In addition, the relative product branching ratio $[\text{H}]/([\text{Cl}]+[\text{Cl}^*])$ and the Cl atom spin-orbit state distribution $[\text{Cl}^*]/[\text{Cl}]$ were determined to be 0.67 ± 0.21 and 0.18 ± 0.04 , respectively.

In this article we report on the extension of our earlier work on the H atom formation in the UV/VUV photolysis of CHF_2Cl (HCFC-22),^{20,21} chloromethanes ($\text{CH}_n\text{Cl}_{4-n}$)²² and $\text{CH}_3\text{CF}_2\text{Cl}$ ¹⁸ towards the direct measurements of absolute Cl atom formation yields via the pulsed laser photolysis (LP)/VUV laser-induced fluorescence (LIF) ‘‘pump-and-probe’’ method. In the present work, the Cl/Cl* fine-structure branching ratio and the absolute Cl atom formation yield $\Phi_{\text{Cl}+\text{Cl}^*}$ in the 193.3 nm photolysis of $\text{CH}_3\text{CF}_2\text{Cl}$ were determined by means of a photolytic calibration method using HCl photolysis as a reference source for well-defined Cl and Cl* atom concentrations. In addition, from the analysis of the measured Cl and Cl* atom Doppler profiles, information about the energy partitioning in the Cl/Cl*-forming photofragmentation step could be derived. A possible primary fragmentation mechanism for $\text{CH}_3\text{CF}_2\text{Cl}$ after photoexcitation at 193.3 nm will be discussed in light of the new results.

II. EXPERIMENT

Photodissociation studies were carried out in a flow cell at mTorr level pressures using the LP/VUV-LIF pump-and-probe setup previously used to study the H atom formation dynamics¹⁹ in the UV and VUV photodissociation of $\text{CH}_3\text{CF}_2\text{Cl}$. A detailed description can be found in Ref. 23. The setup was recently modified to allow VUV-LIF detection of Cl and Cl* atoms produced in bimolecular reactions as described in Ref. 24. In the following only a brief summary of the experimental method will be given.

$\text{CH}_3\text{CF}_2\text{Cl}$ (Messer Griesheim, purity >98%) was pumped through the cell at room temperature. As stated by the manufacturer, the amount of HCFC-141b (CH_3CFCl_2) in the sample was less than 0.1%, with the remaining impurity being CH_3CF_3 which exhibits a negligible absorption at 193.3 nm. The water content was less than 5 ppm. In the

photolysis experiments the $\text{CH}_3\text{CF}_2\text{Cl}$ pressure in the cell was typically 30–45 mTorr. For the calibration measurements, HCl (Messer Griesheim, 99.99%) was flowed through the reaction cell at pressures of typically 7–13 mTorr. $\text{CH}_3\text{CF}_2\text{Cl}$ flow rates were regulated by a calibrated mass flow controller. The HCl flow was regulated by a needle valve. The pressure in the cell was monitored by a MKS-Baratron. Gas flow through the cell was maintained at a high enough rate to ensure renewal of the gas between successive laser shots at a laser repetition rate of 6 Hz.

A UV excimer laser (Lambda Physik LPX 205) operating with an ArF mixture (193.3 nm emission wavelength) was used to photodissociate both the $\text{CH}_3\text{CF}_2\text{Cl}$ parent molecules as well as HCl. A circular aperture was used to skim off the homogeneous part of the rectangular excimer laser profile in order to provide the photolysis beam. A cylindrical lens (1 m focal length) was used to slightly focus the photolysis beam. Pump laser intensities were typically between 4–12 mJ/cm². The analysis of nascent H atom Doppler profiles recorded in the HCl photolysis showed that the pump laser beam was essentially unpolarized [see, e.g., Fig. 2(c) of Ref. 22(a)] and it can therefore be expected that any possible anisotropy of the photodissociation process is averaged out.

For VUV-LIF detection of Cl and Cl* atoms, narrow-band probe laser radiation, tunable in the wavelength region 133.5–136.4 nm was generated using Wallenstein’s method for resonant third-order sum-difference frequency conversion ($\omega_{\text{VUV}}=2\omega_{\text{R}}-\omega_{\text{T}}$) of pulsed dye laser radiation in Krypton.²⁵ In the four-wave mixing process the frequency ω_{R} ($\lambda_{\text{R}}=212.55 \text{ nm}$) is two-photon resonant with the Kr $4p-5p$ (1/2,0) transition. The second frequency ω_{T} could be tuned from 480 to 521 nm to cover the four allowed $\text{Cl}(4s^2P_{j'}\leftarrow 3p^2P_{j''}; j'=1/2,3/2\leftarrow j''=1/2,3/2)$ transitions.²⁶ Ground-state $\text{Cl}(^2P_{3/2})$ and excited-state $\text{Cl}^*(^2P_{1/2})$ atoms were detected via the ($j'=j''$)-transitions, which have the highest transition probabilities $f_{3/2,3/2}=0.114$ and $f_{1/2,1/2}=0.088$, respectively.²⁷ The fundamental laser radiation was obtained from two tunable dye lasers (Lambda Physik FL 2002), simultaneously pumped by a XeCl excimer laser (Lambda Physik EMG 201 MSC). The first dye laser provided ω_{T} by utilizing Coumarin 307 dye. The second dye laser was operated with Coumarin 120 to generate light with a wavelength of 425.10 nm from which ω_{R} was obtained by frequency doubling with a BBO II crystal. The VUV-light generated in the four-wave mixing process was carefully separated from the unconverted laser radiation by a lens monochromator followed by a light baffle system (for details see Ref. 24). The bandwidth of the VUV probe laser radiation ($0.4\text{--}0.5 \text{ cm}^{-1}$) was determined by measuring Doppler profiles of Cl atoms generated in the 193.3 nm photolysis of HCl both under collision-free and thermalized conditions. In the latter case Cl atoms were generated by HCl photolysis in 3 Torr of N_2 and probed after 12 μs . The Cl atom Doppler profiles measured under thermalized conditions could be nicely fit by a Gaussian function indicating that the probe laser lineshape itself can be represented by a Gaussian function. The VUV probe beam was aligned to overlap the photolysis beam at right angles in the viewing region of a LIF detector. The delay time between the photolysis and probe

laser pulses was controlled by a pulse generator and monitored on a fast oscilloscope. The delay time between pumping and probing was kept short enough, typically 80–170 ns (with a time jitter of about ± 10 ns), to allow the collision-free detection of the nascent Cl and Cl* atoms produced in the CH₃CF₂Cl and HCl photolysis. On the other hand, these delay times were long enough to avoid any time-overlap between pump pulse (duration ~ 15 ns) and probe laser pulse (duration ~ 10 ns), which would lead to unwanted multiphoton photochemical processes. Under the described experimental conditions, relaxation of Cl* by quenching as well as fly-out of Cl(Cl*) atoms and secondary reactions with CH₃CF₂Cl and HCl were negligible.

Cl and Cl* LIF signals were measured through a band pass filter (ARC model 130-B-1D; transmission of 29% at 134 nm) by a solar blind photomultiplier (THORN EMI model 9413 B) positioned at right angles to both pump-and-probe laser. The VUV probe beam intensity was monitored after passing through the reaction cell by an additional photomultiplier of the same type. Because the VUV probe beam itself produced an appreciable Cl, Cl* atom LIF signal via photolysis of CH₃CF₂Cl and HCl, respectively, it was necessary to subtract these “background” Cl, Cl* atoms from the Cl, Cl* atoms produced in the 193.3 nm photolysis of CH₃CF₂Cl and HCl. Therefore an electronically controlled mechanical shutter was inserted into the photolysis beam path, such that at each point of the Cl and Cl* spectra, the signal could first be 30 times averaged with the shutter opened and again be 30 times averaged with the shutter closed. Finally a point-by-point subtraction procedure was adopted,²² to obtain directly and on-line a LIF signal representing the contribution from Cl and Cl* atoms generated solely by the 193.3 nm photolysis laser pulse. The Cl, Cl* LIF signals, VUV probe beam and photolysis laser intensity (the latter was monitored by a photodiode) were recorded with a boxcar system and transferred to a microcomputer where the LIF signals were normalized to both pump-and-probe laser intensities. During the experiments special care was taken that the Cl and Cl* atom signals generated by the 193.3 nm photolysis laser pulse showed a linear dependence on the pump and probe laser intensity. Slopes of the linear log–log plots of Cl and Cl* LIF signal intensity against photolysis laser intensity were 0.9 ± 0.1 and 1.1 ± 0.1 , respectively (see, for example, Fig. 1).

III. RESULTS

A. Primary photolytic chlorine atom quantum yield

$\Phi_{\text{Cl}+\text{Cl}^*}$

In order to determine the total chlorine atom quantum yield $\Phi_{\text{Cl}+\text{Cl}^*}$ quantum yields Φ_{Cl} for Cl and Φ_{Cl^*} for Cl* formation were measured separately by calibrating the Cl, Cl* atom signals $S_{\text{Cl}}(\text{CH}_3\text{CF}_2\text{Cl})$, $S_{\text{Cl}^*}(\text{CH}_3\text{CF}_2\text{Cl})$ measured in the CH₃CF₂Cl photodissociation against the Cl, Cl* atom signals $S_{\text{Cl}}(\text{HCl})$, $S_{\text{Cl}^*}(\text{HCl})$ from well-defined Cl, Cl* atom number densities generated in the 193.3 nm photolysis of HCl (see Figs. 2 and 3). Recent kinetics experiments in which the relaxation of Cl* (Cl*+M→M+Cl; M=Ar, N₂, HCl, H₂, D₂, and HD) was investigated, provided a value of

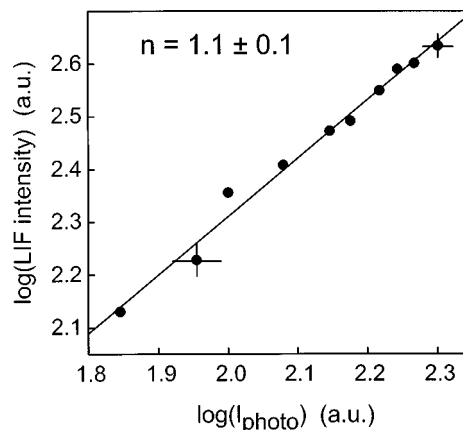


FIG. 1. Dependence of the observed Cl* atom LIF signal from CH₃CF₂Cl photolysis on the photolysis laser intensity. The slope of the fitted linear log–log plot is given in the figure.

0.67 ± 0.09 for the nascent [Cl*]/[Cl] spin-orbit state branching ratio in the 193.3 nm photolysis of HCl.²⁸ This value is within the combined experimental error in good agreement with a value recently reported by Wittig and co-workers.²⁹ Because the 193.3 nm photolysis of HCl generates H+Cl(Cl*) products with a quantum yield of unity ($\phi_{\text{H}} = \phi_{\text{Cl}^*} + \phi_{\text{Cl}} = 1$), values $\phi_{\text{Cl}^*} = 0.40$ and $\phi_{\text{Cl}} = 0.60$ can be derived for the Cl and Cl* fine-structure quantum yields from the [Cl*]/[Cl] ratio.

Quantum yields Φ_{Cl} for Cl and Φ_{Cl^*} for Cl* formation in the 193.3 nm photolysis of CH₃CF₂Cl were determined using Eqs. (1a) and (1b), respectively:

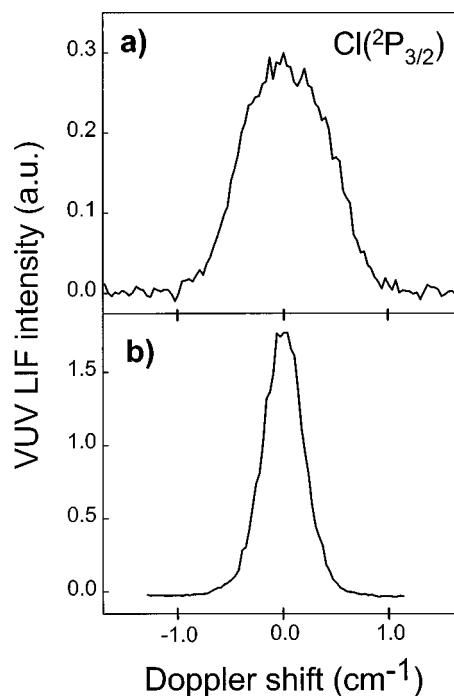


FIG. 2. Doppler profiles of Cl atoms produced in the 193.3 nm laser photolysis of (a) 37 mTorr of CH₃CF₂Cl and (b) 10 mTorr of HCl. The Doppler profiles were recorded 170 ns after the photolysis laser pulse. Line centers correspond to the ($4s\ 2P_{j'=3/2} \leftarrow 3p\ 2P_{j''=3/2}$) transition of the Cl atom (74225.8 cm⁻¹). The laser bandwidth (FWHM) was determined to be 0.42 ± 0.06 cm⁻¹.

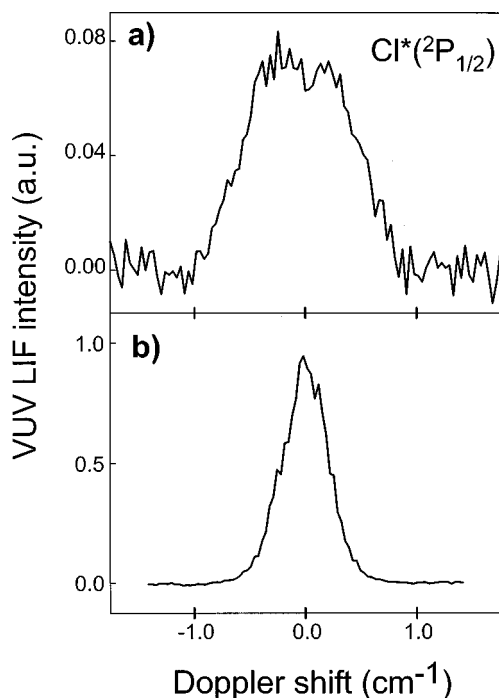


FIG. 3. Doppler profiles of Cl* atoms produced in the 193.3 nm laser photolysis of (a) 37 mTorr of CH₃CF₂Cl and (b) 10 mTorr of HCl. The Doppler profiles were recorded 170 ns after the photolysis laser pulse. Line centers correspond to the ($4s\ ^2P_{j'=1/2} \leftarrow 3p\ ^2P_{j''=1/2}$) transition of the Cl* atom (73983.1 cm^{-1}). The laser bandwidth (FWHM) was determined to be $0.45 \pm 0.07\text{ cm}^{-1}$.

$$\Phi_{\text{Cl}} = \gamma_{\text{Cl}} \{ S_{\text{Cl}}(\text{CH}_3\text{CF}_2\text{Cl}) \phi_{\text{Cl}} \sigma_{\text{HCl}} p_{\text{HCl}} \} / \{ S_{\text{Cl}}(\text{HCl}) \sigma_{\text{CH}_3\text{CF}_2\text{Cl}} p_{\text{CH}_3\text{CF}_2\text{Cl}} \}, \quad (1a)$$

$$\Phi_{\text{Cl}^*} = \gamma_{\text{Cl}^*} \{ S_{\text{Cl}^*}(\text{CH}_3\text{CF}_2\text{Cl}) \phi_{\text{Cl}^*} \sigma_{\text{HCl}} p_{\text{HCl}} \} / \{ S_{\text{Cl}^*}(\text{HCl}) \sigma_{\text{CH}_3\text{CF}_2\text{Cl}} p_{\text{CH}_3\text{CF}_2\text{Cl}} \}. \quad (1b)$$

σ_{HCl} and $\sigma_{\text{CH}_3\text{CF}_2\text{Cl}}$ are the optical absorption cross sections of HCl and CH₃CF₂Cl at $T=295\text{ K}$ and 193.3 nm . S_{Cl} and S_{Cl^*} are the integrated areas under the measured Cl and Cl* atom Doppler profiles and p_{HCl} and $p_{\text{CH}_3\text{CF}_2\text{Cl}}$ are the pressures of HCl and CH₃CF₂Cl, respectively. For the HCl absorption cross sections, we used the value $\sigma_{\text{HCl}} = (8.1 \pm 0.4) \times 10^{-20}\text{ cm}^2$ which has been recently measured for the ArF excimer laser emission wavelength (193.3 nm).³⁰ This value is in good agreement with the value of $8.26 \times 10^{-20}\text{ cm}^2$ which can be obtained by nonlinear interpolation from the recommended data^{31(a)} of Inn.³² For the CH₃CF₂Cl absorption cross section we used the value $\sigma_{\text{CH}_3\text{CF}_2\text{Cl}} = 0.58 \times 10^{-20}\text{ cm}^2$, which represents an average value calculated from the recommended data listed in Ref. 31(a) and the results of the most recent measurements by Nayak *et al.*³³ The uncertainty of the CH₃CF₂Cl absorption cross section at 193.3 nm was estimated to be $\pm 5\%$ based on the scatter of the data reported in Refs. 33–36 for the $180\text{--}200\text{ nm}$ region.

The factors γ_{Cl^*} , γ_{Cl} in Eqs. (1a) and (1b) are corrections accounting for the different degrees of absorption of the Cl ($\gamma_{\text{probe}} \approx 134.72\text{ nm}$) and Cl* ($\lambda_{\text{probe}} \approx 135.16\text{ nm}$) VUV probe laser radiation by CH₃CF₂Cl and HCl, respectively. The absorption corrections could be directly determined

from the known distances inside the flow cell and the relative difference in the VUV probe laser attenuation measured in the CH₃CF₂Cl photolysis and HCl calibration runs. Under typical experimental conditions ($p_{\text{CH}_3\text{CF}_2\text{Cl}} = 30\text{ mTorr} = 3 \times p_{\text{HCl}}$) the absorption corrections were $\gamma_{\text{Cl}} = 0.87 \pm 0.04$ and $\gamma_{\text{Cl}^*} = 0.86 \pm 0.04$. The experimental data set evaluated via Eq. (1a) to determine Φ_{Cl} consisted of ten Cl atom profiles obtained in combination with ten Cl profiles from HCl calibration runs. The Cl* atom quantum yield was evaluated via Eq. (1b) in the same manner. The quoted errors were determined from the 1σ statistical uncertainties of the experimental data, the uncertainties of the CH₃CF₂Cl and HCl optical absorption cross sections and the uncertainty of the $[\text{Cl}^*]/[\text{Cl}]$ value in the 193.3 nm photolysis of HCl using simple error propagation. The following values for the Cl and Cl* atom quantum yields were obtained: $\Phi_{\text{Cl}}(193.3\text{ nm}) = 0.65 \pm 0.12$ and $\Phi_{\text{Cl}^*}(193.3\text{ nm}) = 0.25 \pm 0.05$ leading to a value of $\Phi_{\text{Cl}+\text{Cl}^*}(193.3\text{ nm}) = 0.90 \pm 0.17$ for the total quantum yield. From the measured Cl and Cl* atom quantum yields, the spin-orbit branching ratio of the Cl fragment in the 193.3 nm photolysis of CH₃CF₂Cl can be calculated: $[\text{Cl}^*]/[\text{Cl}] = 0.39 \pm 0.11$.

B. Average Cl atom translational energy

The measured Cl atom spectral profiles were analyzed in order to determine the average kinetic energy of the fragments in the CH₃CF₂Cl photolysis. The Doppler profiles directly reflect, via the linear Doppler shift $[\nu - \nu_0]/\nu_0 = v_z/c$, the distribution $f(v_z)$ of the velocity component v_z of the absorbing atoms along the propagation direction of the probe laser beam. Hence, for an isotropic velocity distribution the average Cl atom kinetic energy in the laboratory system is given by $E_{\text{Lab}(\text{Cl})} = 3/2 m_{\text{Cl}} \langle v_z^2 \rangle$, where $\langle v_z^2 \rangle$ represents the second moment of the laboratory velocity distribution $f(v_z)$ of the photolytically produced Cl atoms. However, since the measured spectral profiles represent a convolution of the laser spectral profile and the Doppler profile of the absorbing Cl atoms, a deconvolution was carried out to obtain the correct Cl velocity distribution $f(v_z)$ using a Gaussian function to describe the VUV laser spectral profile. The width of the laser spectral profile was determined from Cl (Cl*) profiles measured in the HCl photolysis [see, e.g., Figs. 2(b) and 3(b)] recorded right after the Cl (Cl*) profiles from the CH₃CF₂Cl photolysis [see, e.g., Figs. 2(a) and 3(a)]. Evaluation of the complete set of 20 experimental Cl (Cl*) profiles taking into account the actual laser bandwidth revealed that the kinetic energies of both fragments in the CH₃CF₂Cl photolysis are the same within the experimental uncertainty ($E_{\text{Lab}(\text{Cl})} \approx E_{\text{Lab}(\text{Cl}^*)}$). Calculation of the second moments of $f(v_z)$ gave an average value of $E_{\text{Lab}(\text{Cl})} = 82 \pm 16\text{ kJ/mol}$ for the laboratory kinetic energy of the fragments. The quoted error includes the 1σ statistical uncertainties obtained in the individual fits used to evaluate the experimental spectral profiles from CH₃CF₂Cl and the HCl photolysis using error propagation. The corresponding relative kinetic energy in the Cl–CH₃CF₂ center-of-mass (cm) system was calculated to be $E_{\text{cm}} = 125 \pm 25\text{ kJ/mol}$.

IV. DISCUSSION

Absorption of a 193.3 nm photon by a $\text{CH}_3\text{CF}_2\text{Cl}$ molecule leads to an excitation in the first absorption band [denoted as A band in Ref. 11(a)]. “A band absorption” originates from a $3p\pi \rightarrow \sigma^*$ (C–Cl) transition within the valence shell, where $3p\pi$ is a Cl lone pair orbital and σ^* is an antibonding C–Cl σ -MO. Therefore it is expected that the initial excitation is localized in the C–Cl bond^{11(c)} leading preferentially to the breaking of this bond.^{31(a)} Furthermore the A band of $\text{CH}_3\text{CF}_2\text{Cl}$ is structureless,^{11(b)} suggesting a direct dissociation mechanism.³⁷

A. Primary chlorine release channels and energy disposal

The present result for the primary photolytic chlorine atom quantum yield suggests that the chlorine contents of room-temperature $\text{CH}_3\text{CF}_2\text{Cl}$, after photoexcitation at 193.3 nm under collision-free conditions, is released to a large extent as atomic chlorine. The value for the chlorine atom quantum yield measured in the present work is consistent with the earlier measured H atom quantum yield¹⁸ of $\Phi_{\text{H}}(193.3 \text{ nm}) = 0.06 \pm 0.02$ and with the upper limit for the HCl quantum yield reported in Ref. 19. In the latter experiments, no $\text{HCl}(v''=0,1)$ product molecules could be observed and the quantum yield was estimated to be $\Phi_{\text{HCl}(v''=0,1)}(193.3 \text{ nm}) < 0.01$. However, IRMPD experiments revealed that in the four-center elimination, a large fraction of the total excess energy (>85%) is left as internal excitation of the $\text{CH}_2=\text{CF}_2$ and HCl fragments and it was suggested that the HCl fragments must be highly vibrationally excited.¹⁴ As a consequence, the actual HCl yield in the 193.3 nm photolysis of $\text{CH}_3\text{CF}_2\text{Cl}$ could be considerably higher than the upper limit estimated in Ref. 19 from the absence of $\text{HCl}(v''=0,1)$ products. The result of the present work puts an upper limit of $\Phi_{\text{HCl}}(193 \text{ nm}) < 0.27$ for the total HCl quantum yield. Hence, to fully elucidate the dynamics of a possible HCl formation channel after UV excitation, further studies are clearly needed which should include detection of $\text{HCl}(v'' > 1)$ product vibrational states. HCl elimination has been observed in the 193.3 nm photolysis of $\text{CH}_3\text{CH}_2\text{Cl}$ and attributed to a mechanism which involves internal conversion to the electronic ground state.³⁸

The average Cl translational energy determined in the present work corresponds to a value of $f_T = E_{\text{cm}}/E_{\text{avt}} = 0.48 \pm 0.10$. This value is—within experimental uncertainty—in agreement with the value of $f_T = 0.39$ calculated using a repulsive model.³⁹ This confirms that formation of chlorine atoms proceeds predominantly by a direct dissociation mechanism on a PES that is repulsive along the C–Cl bond coordinate.

B. Chlorine atom spin-orbit branching ratio

Accurate measurements of spin-orbit branching ratios $[\text{X}^*(^2P_{1/2})]/[\text{X}(^2P_{3/2})]$ of halogen atoms (X=Cl, Br, I) produced in the photodissociation of halogenated compounds play an important role in the elucidation of the influence of nonadiabatic couplings on molecular dynamics.^{40,41} However, even for HCl as one of the simplest systems, the

$[\text{Cl}^*]/[\text{Cl}]$ branching ratio from photodissociation out of the ground vibrational state was for a considerable time subject to controversy.^{42,43} A recent study of the 193.3 nm photodissociation of HCl by Wittig and co-workers, in which the high-*n* Rydberg time-of-flight (HRTOF) technique was utilized to record H atom product TOF spectra, yielded a value of $[\text{Cl}^*]/[\text{Cl}] = 0.69 \pm 0.02$.²⁹ This value was found to be in excellent agreement with the theoretical value of 0.71 calculated for the 193.3 nm excitation wavelength.⁴⁴ In a recent experimental and theoretical study, spin-orbit branching in the HCl photolysis was investigated at long excitation wavelengths (193.3–235.3 nm).⁴⁵ The experimental spin-orbit branching ratios, obtained by (2+1) REMPI using the $4p\ ^2D_{3/2} \leftarrow 3p\ ^2P_{3/2}$ two-photon transition for Cl and the $4p\ ^2D_{3/2} \leftarrow 3p\ ^2P_{1/2}$ and $4p\ ^2P_{1/2} \leftarrow 3p\ ^2P_{1/2}$ two-photon transitions for Cl^* detection, were found to be in good agreement with the theoretical results only after scaling to agree with the Wittig value at 193.3 nm.⁴⁶ As a consequence, we tend to believe that the latter one can serve as a general calibration point for the measurement of Cl atom spin-orbit branching ratios, in particular because it has been determined by a technique which is independent of the detection efficiency of Cl and Cl^* atoms.

The value $[\text{Cl}^*]/[\text{Cl}] = 0.39 \pm 0.11$ determined in the present investigation for the 193.3 nm photolysis of $\text{CH}_3\text{CF}_2\text{Cl}$ was obtained by calibrating the Cl and Cl^* VUV-LIF signals against those obtained in the HCl photolysis. In Ref. 19, a significant lower value of $[\text{Cl}^*]/[\text{Cl}] = 0.18 \pm 0.04$ was reported for the 193.3 nm photolysis of $\text{CH}_3\text{CF}_2\text{Cl}$ in a molecular beam using the (2+1) REMPI method for Cl and Cl^* detection. The latter value was obtained using the “old” HCl chlorine branching ratio $[\text{Cl}^*]/[\text{Cl}] = 0.50$ as a reference.⁴³ Rescaling using the new HCl chlorine branching ratio of Wittig *et al.*²⁹ changes the value to $[\text{Cl}^*]/[\text{Cl}] = 0.24 \pm 0.05$ and brings it closer to the result of the present work.

Spin-orbit branching of atomic products is usually governed by the nature of the PES(s) excited in the Franck–Condon region as well as by subsequent nonadiabatic couplings between the surfaces as the products depart. As a result, for the correct interpretation of measured spin-orbit branching ratios, information is required about the PESs involved in the initial optical excitation and subsequent fragmentation process. Although such information is so far not available for $\text{CH}_3\text{CF}_2\text{Cl}$, comparison can be made with CH_3Cl for which more detailed spectroscopic and dynamical data is available. For CH_3Cl it was found that photoabsorption at 193.3 nm is associated with a parallel transition from the $\bar{X}\ ^1A_1$ ground state to the 3Q_0 state, which correlates diabatically with Cl^* products. The observed Cl formation was attributed to a level crossing of the 3Q_0 potential curve by the electronically excited 1Q_1 state which diabatically correlates with Cl products. Therefore the $[\text{Cl}^*]/[\text{Cl}]$ branching ratios should depend on the relative velocity of the product fragments while the system passes through the crossing region and the $[\text{Cl}^*]/[\text{Cl}]$ branching ratio is expected to increase in going to shorter photolysis wavelengths. Such a behavior was indeed observed in Ref. 47 where $[\text{Cl}^*]/[\text{Cl}]$ branching ratios of 0.27 ± 0.01 and 0.62 ± 0.06 were reported

for photolysis wavelengths of 235 and 193.3 nm, respectively. Assuming that for both $\text{CH}_3\text{CF}_2\text{Cl}$ and CH_3Cl , the spin-orbit branching is determined as the fragments separate (and not in the initial excitation), the higher $[\text{Cl}^*]/[\text{Cl}]$ branching ratio observed in the 193.3 nm photolysis of CH_3Cl can be attributed to the higher relative velocity of the separating fragments. For the CH_3+Cl fragments, a relative velocity of 6300 m/s can be calculated from the f_T value of 0.78 reported in Ref. 48, while the present work yields a value of 3200 m/s for the $\text{CH}_3\text{CF}_2+\text{Cl}$ fragments. Hence the CH_3+Cl fragmentation process should be more diabatic leading to a higher amount of Cl^* fragments formed on the initially excited 3Q_0 PES.

C. H atom formation dynamics and $[\text{H}]/[\text{Cl}+\text{Cl}^*]$ branching ratio

In a study of the H atom formation dynamics in the 193.3 nm laser photolysis of room-temperature $\text{CH}_3\text{CF}_2\text{Cl}$, a value of $\Phi_{\text{H}}(193.3 \text{ nm}) = 0.06 \pm 0.02$ was reported for the H atom product quantum yield and the relative translational energy of the H atom fragments was determined to be $E_{T(\text{H})}(193.3 \text{ nm}) = 51 \pm 10 \text{ kJ/mol}$.¹⁸ From the results of our earlier H atom study and the present Cl^* and Cl atom quantum yield measurements a $[\text{H}]/[\text{Cl}+\text{Cl}^*]$ branching ratio of 0.07 ± 0.03 can be calculated. Comparison of Eq. (1) of the present paper which was used to determine $\Phi_{\text{Cl}+\text{Cl}^*}$ with the corresponding Eq. (1) for Φ_{H} in Ref. 18 shows that the actual values of the HCl and $\text{CH}_3\text{CF}_2\text{Cl}$ optical absorption cross sections are not needed if one wants to determine only the relative branching ratio $[\text{H}]/[\text{Cl}+\text{Cl}^*] = \Phi_{\text{H}}/\Phi_{\text{Cl}+\text{Cl}^*}$. In that case the HCl photolysis measurements serve as a calibration of the relative H versus Cl atom LIF detection efficiency. Hence the above $[\text{H}]/[\text{Cl}+\text{Cl}^*]$ branching ratio can be directly compared with the results of Ref. 19 in which H atoms were observed during 193.3 nm laser photolysis of a ‘‘cold’’ molecular beam of neat $\text{CH}_3\text{CF}_2\text{Cl}$. Here the H atoms were detected by (2+1) REMPI via the $2s^2S \leftarrow 1s^2S$ two-photon transition around 243.135 nm and the $4p^2D_{3/2} \leftarrow 3p^2P_{3/2}$ and $4p^2D_{3/2} \leftarrow 3p^2P_{1/2}$ two-photon transitions were utilized for Cl and Cl^* atom (2+1) REMPI detection, respectively. In this study a relative $[\text{H}]/[\text{Cl}+\text{Cl}^*]$ branching ratio of 0.67 ± 0.21 was measured using HCl photolysis to calibrate the H versus Cl atom REMPI detection efficiency.¹⁹ The same experiments yielded an average value of $E_{T(\text{H})}(193.3 \text{ nm}) = 91 \pm 19 \text{ kJ/mol}$ for the H atom translational energy. Both values are significantly higher than those obtained in the room temperature gas-phase photolysis experiments. On the other hand, the Cl atom translational energy release seems to be reduced compared to the gas-phase results.⁴⁹ The difference between the molecular beam and the gas-phase results could indicate that cooling of the parent molecules leads to a significant modification of the product branching and fragmentation dynamics.

For the molecular beam studies of Ref. 19, a $\text{CH}_3\text{CF}_2\text{Cl}$ rotational temperature of 100 K was reported. Based on this, one can estimate that under the conditions of the molecular beam experiment (assuming $T_{\text{vib}} \approx T_{\text{rot}}$) only a small fraction (ca. 4%) of the $\text{CH}_3\text{CF}_2\text{Cl}$ molecules are in vibrational levels with $v > 0$, while for a room temperature sample this value is

considerably higher (ca. 70%).^{50,51} As a consequence of the markedly different parent molecule vibrational state distributions in the molecular beam and the room temperature gas phase experiments, UV photon absorption could lead (due to a different Franck–Condon overlap between the ground vibronic and the electronically excited states wave functions) to the excitation of different PESs. The assessment of different electronically excited PESs or—in the case that only one electronically excited PES is involved—the assessment of different regions of the excited PES could be one possible explanation of the observed difference in the dissociation dynamics. However, further theoretical work on the electronically excited molecular state(s) structure in combination with additional experimental work in the gas-phase and under well-characterized molecular beam conditions is needed before a more detailed picture of the H atom formation dynamics can be drawn. On the experimental side, measurements of the product state distributions of the $\text{CH}_2\text{CF}_2\text{Cl}$, and CH_2CF_2 co-fragments and the investigation of vector correlations for different photolysis wavelengths would be most useful in helping to identify the excited electronic state(s) involved in the UV photolysis of $\text{CH}_3\text{CF}_2\text{Cl}$.

V. SUMMARY

In a gas-phase laser photolysis/laser-induced fluorescence ‘‘pump-and-probe’’ study absolute quantum yields for photolytic formation of Cl^* and Cl atoms were determined after UV laser excitation of room-temperature $\text{CH}_3\text{CF}_2\text{Cl}$ (HCFC-142b) at 193.3 nm. In agreement with our earlier H atom quantum yield measurements,¹⁸ which gave a value of $\Phi_{\text{H}}(193.3 \text{ nm}) = 0.06 \pm 0.02$, the value of $\Phi_{\text{Cl}+\text{Cl}^*} = 0.90 \pm 0.17$ obtained in the present work clearly indicates that C–Cl bond cleavage is the dominant dissociation pathway after A band excitation. The fraction of total available energy channeled into $\text{CH}_3\text{CF}_2+\text{Cl}$ product translational energy was found to be in agreement with the result of a dynamical simulation assuming a repulsive model for single C–Cl bond cleavage. Both the measured total Cl atom quantum yield and the energy disposal indicates that direct C–Cl bond cleavage is a primary fragmentation mechanism for $\text{CH}_3\text{CF}_2\text{Cl}$ after photoexcitation at 193.3 nm.

ACKNOWLEDGMENTS

The authors gratefully acknowledge financial support of the European Union (Contract No. ISC*-CT940096 of the International Scientific Cooperation program between the University of Heidelberg and the Ben-Gurion-University of the Negev, Beer-Sheva, Israel), the Korea Research Foundation (nondirected research fund 1995–1998), and the Korea Science and Engineering Foundation (Korea-Germany Joint Project, 1997–1998). HPU wishes to acknowledge a fellowship provided by the DLR Bonn (Indo-German bilateral agreement, Project No. CHEM-19). HRV would like to thank I. Bar, A. Melchior, S. Rosenwaks, M. Cameron, and R. K. Vatsa for helpful communications and J. Wolfrum (Director of the Institute of Physical Chemistry, Ruprecht-Karls-University Heidelberg) for his continuous support and his interest in the ongoing work.

- ¹P. J. Crutzen, in *Physics and Chemistry of Upper Atmospheres*, edited by B. M. McCormac (Reidel, Dordrecht, 1973); M. J. Molina and F. S. Rowland, *Nature (London)* **249**, 810 (1974).
- ²R. P. Wayne, *The Chemistry of Atmospheres*, 2nd ed. (Oxford University Press, Oxford, 1991) and references therein.
- ³*ATLAS3 Public Affairs Status Report #20*, NASA Science Operation Space Flight Center, Huntsville, Nov. 13, 1994.
- ⁴A. K. Nayak, T. J. Buckley, M. J. Kurylo, and A. Fahr, *J. Geophys. Res.* **101**, 9055 (1996).
- ⁵S. Pinnock, M. D. Hurley, K. P. Shine, T. J. Wallington, and T. J. Smyth, *J. Geophys. Res.* **100**, 23227 (1995).
- ⁶E. Linak and P. Yau, *Chemical Economics Handbook* (SRI International, Menlo Park, CA, 1995).
- ⁷J. M. Lee, W. T. Sturges, S. A. Penkett, D. E. Oram, U. Schmidt, A. Engel, and R. Bauer, *Geophys. Res. Lett.* **22**, 1369 (1995).
- ⁸T. Shirai and Y. Makide, *Chem. Lett.* **4**, 357 (1998).
- ⁹M. Kanakidou, F. J. Dentener, and P. J. Crutzen, *J. Geophys. Res.* **100**, 18781 (1995).
- ¹⁰*Scientific Assessment of Ozone Depletion: 1991*, World Meteorological Organization Global Research and Monitoring Project Report No. 25 (World Meteorological Organization, Geneva, Switzerland, 1992).
- ¹¹(a) M. B. Robin, *Higher Excited States of Polyatomic Molecules*, Vol. I (Academic, New York, 1974); (b) J. Doucet, P. Sauvageau, and C. Sander, *J. Chem. Phys.* **62**, 355 (1975); (c) H. Okabe, *Photochemistry of Small Molecules* (Wiley, New York, 1978); (d) W. B. DeMore, S. P. Sander, D. M. Golden, R. F. Hampson, M. J. Kurylo, C. J. Howard, A. R. Ravishankara, C. E. Kolb, and M. J. Molina, *Chemical Kinetics and Photochemical Data for Use in Stratospheric Modeling*, No. 12 (NASA, JPL Publication 97-4, 1997).
- ¹²For example, Z. F. Dong, M. Schneider, and J. Wolfrum, *Int. J. Chem. Kinet.* **21**, 387 (1989) and references therein.
- ¹³For example, Y. Jones, B. E. Homes, D. W. Duke, and D. L. Tipton, *J. Phys. Chem.* **94**, 4957 (1990) and references therein.
- ¹⁴R. N. Zitter and D. F. Koster, *J. Am. Chem. Soc.* **100**, 2265 (1978); R. N. Zitter, D. F. Koster, A. Cantoni, and J. Pleil, *Chem. Phys.* **46**, 107 (1980); R. N. Zitter, D. F. Koster, A. Cantoni, and A. Ringwelski, *Chem. Phys.* **51**, 11 (1981).
- ¹⁵A. S. Sudbo, P. A. Schulz, E. R. Grant, Y. R. Shen, and Y. T. Lee, *J. Chem. Phys.* **68**, 1306 (1978); A. S. Sudbo, P. A. Schulz, Y. R. Shen, and Y. T. Lee, *J. Chem. Phys.* **69**, 2312 (1978); G. A. West, R. E. Weston, Jr., and G. W. Flynn, *Chem. Phys.* **35**, 275 (1978); A. Sondag and G. H. Wegdam, *Chem. Phys. Lett.* **92**, 191 (1982).
- ¹⁶T. Ichimura, A. W. Kirk, and E. Tschuikow-Roux, *J. Phys. Chem.* **81**, 2040 (1977).
- ¹⁷T. Ichimura, A. W. Kirk, and E. Tschuikow-Roux, *Int. J. Chem. Kinet.* **9**, 697 (1977).
- ¹⁸R. A. Brownsword, M. Hillenkamp, T. Laurent, H.-R. Volpp, J. Wolfrum, R. K. Vatsa, and H.-S. Yoo, *J. Chem. Phys.* **107**, 779 (1997).
- ¹⁹(a) A. Melchior, I. Bar, and S. Rosenwaks, *J. Chem. Phys.* **107**, 8476 (1997); (b) A. Melchior, H. M. Lambert, P. J. Dagdigian, I. Bar, and S. Rosenwaks, *Isr. J. Chem.* **37**, 455 (1997); A comparison of Fig. 1 of Ref. 19 (a) with the data shown in Fig. 2 of Ref. 19 (b) suggests that the H and Cl atom REMPI signals obtained for CH₃CF₂Cl (HCFC-142b) have been erroneously assigned to CH₃CFCl₂ (HCFC-141b) in the latter article.
- ²⁰A. Melchior, P. Knupfer, I. Bar, S. Rosenwaks, T. Laurent, H.-R. Volpp, and J. Wolfrum, *J. Phys. Chem.* **100**, 13375 (1996).
- ²¹R. A. Brownsword, M. Hillenkamp, T. Laurent, R. K. Vatsa, H.-R. Volpp, and J. Wolfrum, *J. Phys. Chem. A* **101**, 995 (1997).
- ²²(a) R. A. Brownsword, M. Hillenkamp, T. Laurent, R. K. Vatsa, H.-R. Volpp, and J. Wolfrum, *J. Phys. Chem. A* **101**, 5222 (1997); (b) R. A. Brownsword, M. Hillenkamp, T. Laurent, R. K. Vatsa, H.-R. Volpp, and J. Wolfrum, *J. Chem. Phys.* **106**, 1359 (1997).
- ²³R. A. Brownsword, M. Hillenkamp, T. Laurent, R. K. Vatsa, and H. R. Volpp, *J. Chem. Phys.* **106**, 4436 (1997).
- ²⁴R. A. Brownsword, C. Kappel, P. Schmiechen, H. P. Upadhyaya, and H.-R. Volpp, *Chem. Phys. Lett.* **289**, 241 (1998).
- ²⁵G. Hilber, A. Lago, and R. Wallenstein, *J. Opt. Soc. Am. B* **4**, 1753 (1987).
- ²⁶K. Tonokura, Y. Matsumi, M. Kawasaki, S. Tasaki, and R. Bersohn, *J. Chem. Phys.* **97**, 8210 (1992) and references therein.
- ²⁷W. L. Wiese, M. W. Smith, and B. M. Miles, *Atomic Transition Probabilities*, Vol. 2, Nat. Stand. Ref. Data Ser. Nat. Bur. Stand. 22 (1969).
- ²⁸R. A. Brownsword, C. Kappel, H. P. Upadhyaya, and H.-R. Volpp (to be published).
- ²⁹J. Zhang, M. Dulligan, and C. Wittig, *J. Chem. Phys.* **107**, 1403 (1997).
- ³⁰Y. Mo, K. Tonkua, Y. Matsumi, M. Kawasaki, T. Sato, T. Arikawa, P. T. A. Reilly, Y. Xie, Y. Yag, Y. Huang, and R. J. Gordon, *J. Chem. Phys.* **97**, 4815 (1992).
- ³¹(a) R. Atkinson, D. L. Baulch, R. A. Cox, R. F. Hampson, Jr., J. A. Kerr, and J. Troe, *J. Phys. Chem. Ref. Data* **21**(6), 1125 (1992); (b) C. F. Melius, Sandia National Laboratories, BAC-MP4 Heats of Formation Data File (Vers. July 16, 1996).
- ³²E. C. Y. Inn, *J. Atmos. Sci.* **32**, 2375 (1975).
- ³³(a) R. A. Brownsword, M. J. Kurylo, and A. Fahr, *J. Geophys. Res.* **101**, 9055 (1996).
- ³⁴C. Hubrich and F. Stuhl, *J. Photochem.* **12**, 93 (1980).
- ³⁵D. Gillotay and P. C. Simon, *J. Atmos. Chem.* **12**, 269 (1991).
- ³⁶R. Talukdar, A. Mellouki, T. Gierczak, J. B. Burkholder, S. A. McKeen, and A. R. Ravishankara, *J. Phys. Chem.* **95**, 5815 (1991).
- ³⁷(a) R. Bersohn, in *Molecular Photodissociation Dynamics*, edited by M. N. R. Ashfold and J. E. Baggot (Royal Society of Chemistry, London, 1987); (b) R. Schinke, *Photodissociation Dynamics* (Cambridge University Press, Cambridge, 1992).
- ³⁸M. Kawasaki, K. Kasatani, H. Sato, H. Shinohara, and N. Nishi, *Chem. Phys.* **88**, 135 (1984).
- ³⁹A. F. Tuck, *J. Chem. Soc., Faraday Trans. 2* **73**, 689 (1977).
- ⁴⁰R. D. Levine and R. B. Bernstein, *Molecular Reaction Dynamics and Chemical Reactivity* (Oxford University Press, Oxford, 1987).
- ⁴¹R. N. Dixon, *Chem. Soc. Rev.* **23**, 375 (1994).
- ⁴²Y. Matsumi, K. Tonokura, M. Kawasaki, and T. Ibuki, *J. Chem. Phys.* **93**, 7981 (1990).
- ⁴³Y. Matsumi, K. Tonokura, M. Kawasaki, and T. Ibuki, *J. Chem. Phys.* **97**, 5261 (1992).
- ⁴⁴M. H. Alexander, B. Pouilly, and T. Duhoo, *J. Chem. Phys.* **99**, 1752 (1993).
- ⁴⁵H. M. Lambert, P. J. Dagdigian, and M. H. Alexander, *J. Chem. Phys.* **108**, 4460 (1998).
- ⁴⁶The authors of Ref. 45 noted that the use of the ratio of the REMPI line intensities reported in Ref. 43 would lead to 35% lower values.
- ⁴⁷H. M. Lambert and P. J. Dagdigian, *Chem. Phys. Lett.* **275**, 499 (1997).
- ⁴⁸Y. Matsumi, K. Tonokura, M. Kawasaki, G. Inoue, S. Satyapal, and R. Bersohn, *J. Chem. Phys.* **94**, 2669 (1991).
- ⁴⁹From the Cl atom Doppler width (FWHM=0.55 cm⁻¹) reported in Ref. 19(a) the average relative kinetic energy can be estimated (assuming a VUV effective laser bandwidth of 0.4 cm⁻¹) to be ca. 28 kJ/mol which is about 4.5 times smaller than the average relative Cl fragment kinetic energy determined in the present room temperature gas phase experiments.
- ⁵⁰D. McNaughton and C. Evans, *J. Mol. Spectrosc.* **182**, 342 (1997).
- ⁵¹The relative population of the vibrationally excited states was estimated treating the CH₃CF₂Cl molecule as a quantum mechanical harmonic oscillator with 18 normal modes of vibration. The values for the 18 vibrational frequencies were taken from Ref. 50.